



Scaling and maintenance of corneal thickness during aging

Citation

Inomata, Takenori, Alireza Mashaghi, Jiaxu Hong, Takeshi Nakao, and Reza Dana. 2017. "Scaling and maintenance of corneal thickness during aging." PLoS ONE 12 (10): e0185694. doi:10.1371/journal.pone.0185694. <http://dx.doi.org/10.1371/journal.pone.0185694>.

Published Version

doi:10.1371/journal.pone.0185694

Permanent link

<http://nrs.harvard.edu/urn-3:HUL.InstRepos:34492177>

Terms of Use

This article was downloaded from Harvard University's DASH repository, and is made available under the terms and conditions applicable to Other Posted Material, as set forth at <http://nrs.harvard.edu/urn-3:HUL.InstRepos:dash.current.terms-of-use#LAA>

Share Your Story

The Harvard community has made this article openly available.
Please share how this access benefits you. [Submit a story](#).

[Accessibility](#)

RESEARCH ARTICLE

Scaling and maintenance of corneal thickness during aging

Takenori Inomata^{1,2}, Alireza Mashaghi^{1,3}, Jiaxu Hong¹, Takeshi Nakao¹, Reza Dana^{1*}

1 Schepens Eye Research Institute, Massachusetts Eye and Ear Infirmary, Department of Ophthalmology, Harvard Medical School, Boston, MA, United States of America, **2** Juntendo University Faculty of Medicine, Department of Ophthalmology, Tokyo, Japan, **3** Leiden Academic Centre for Drug Research, Faculty of Mathematics and Natural Sciences, Leiden University, Leiden, The Netherlands

These authors contributed equally to this work.

* Reza_Dana@meei.harvard.edu



Abstract

Corneal thickness is tightly regulated by its boundary endothelial and epithelial layers. The regulated set-point of corneal thickness likely shows inter-individual variations, changes by age, and response to stress. Using anterior segment-optical coherence tomography, we measure murine central corneal thickness and report on body size scaling of murine central corneal thickness during aging. For aged-matched mice, we find that corneal thickness depends on sex and strain. To shed mechanistic insights into these anatomical changes, we measure epithelial layer integrity and endothelial cell density during the life span of the mice using corneal fluorescein staining and *in vivo* confocal microscopy, respectively and compare their trends with that of the corneal thickness. Cornea thickness increases initially (1 month: $114.7 \pm 3.0 \mu\text{m}$, 6 months: $126.3 \pm 1.6 \mu\text{m}$), reaches a maximum (9 months: $129.3 \pm 4.4 \mu\text{m}$) and then reduces (12 months: $127 \pm 2.9 \mu\text{m}$, 13 months: $119.5 \pm 7.6 \mu\text{m}$, 14 months: $110.6 \pm 10.6 \mu\text{m}$), while the body size (weight) increases with age. We find that endothelial cell density reduces from 2 months old to 8 months old as the mice age and epithelial layer accumulates damages within this time frame. Finally, we compare murine corneal thickness with those of several other mammals including humans and show that corneal thickness has an allometric scaling with body size. Our results have relevance for organ size regulation, translational pharmacology, and veterinary medicine.

OPEN ACCESS

Citation: Inomata T, Mashaghi A, Hong J, Nakao T, Dana R (2017) Scaling and maintenance of corneal thickness during aging. PLoS ONE 12(10): e0185694. <https://doi.org/10.1371/journal.pone.0185694>

Editor: Alexander V. Ljubimov, Cedars-Sinai Medical Center, UNITED STATES

Received: December 28, 2016

Accepted: September 18, 2017

Published: October 6, 2017

Copyright: © 2017 Inomata et al. This is an open access article distributed under the terms of the [Creative Commons Attribution License](https://creativecommons.org/licenses/by/4.0/), which permits unrestricted use, distribution, and reproduction in any medium, provided the original author and source are credited.

Data Availability Statement: All relevant data are within the paper and its Supporting Information files.

Funding: This study was supported by the National Institutes of Health grant EY20889 (RD) and National Institutes of Health grant EY12963 (RD).

Competing interests: The authors have declared that no competing interests exist.

Introduction

Size is a critical property of biological systems and is tightly regulated [1]. Body size determines the metabolic rate of organisms [2, 3], interactions of organisms with their environment [4, 5] and is related to biological diversity and population size [6]. How does body size relate to the size of internal organs, what determines size of internal organs, and how internal organs respond to environmental stresses are fundamental questions in biology [7–9].

Allometry, a term coined by Julian Huxley and Georges Tessier in 1936, applies to the phenomenon of relative growth. Organs may have higher growth rate than the whole body (positive allometry), identical growth rate with the whole body (isometry) or lower relative growth rate (negative allometry) [10]. It is noteworthy that studies on allometry are not limited to

analyzing age-related changes, the so-called ontogenetic allometry, but also include analysis of inter-individual and inter-species size variations, termed as static and evolutionary allometry respectively.

The eye has been subject to allometric analysis. Axial length of vertebrate eyes obeys a logarithmic relationship with body weight with a negative allometric scaling [11]. Visual organs in human grow to its 80% of adult size by age 4 [12]. Early in life, the orbit size changes with age and doubles its birth weight by 7–8 years of age when it reaches the adult size [13]. The size of an emmetropic human adult eye does not depend on sex or age [14]. Whether eye components also follow size rules similar to the whole eye remains to be studied.

The cornea forms the anterior segment of the eye and is the eye's primary light-focusing structure. Here, we ask how central cornea thickness changes during development and aging in laboratory mouse and how it scales with body size. We determine how the scaling is affected by sex, and how it depends on species. Finally, we perform a systematic literature study and compare body size scaling of murine corneal thickness to several other mammals including humans.

Materials and methods

Mice, husbandry and anesthesia

1–14 month old C57BL/6 (H-2b) and BALB/c (H-2d) female and male mice were purchased from Charles River Laboratories (Wilmington, MA, USA). Mice were housed in a specific pathogen-free environment at the Schepens Eye Research Institute animal facility. They were aged in our AAALAC-certified vivarium in a standard 12:12-hour light–dark cycle and fed irradiated diet (Teklad global 19% protein extruded Rodent Diet 2918, Harlan Laboratories, Indianapolis, IN, USA). Mice were weighed by weight scale.

Anesthesia was administered intraperitoneally by ketamine/xylazine solution at a dose of 120 mg/kg body weight and 20 mg/kg body weight, respectively. Under these conditions, the eyes of mice are naturally wide open and in a stable position, with pupils pointing laterally and upward.

All animals were treated according to the guidelines established by the Association for Research in Vision and Ophthalmology (ARVO) Statement for the Use of Animals in Ophthalmic and Vision Research and Public Health Review, and all procedures were approved by the Institutional Animal Care and Use Committee of the Schepens Eye Research Institute.

Corneal thickness measurement

Images of the anterior segment were taken by anterior segment-optical coherence tomography (AS-OCT; Bioptigen, Durham, NC, USA) in order to determine the corneal thickness. For high resolution central corneal cross-sectional scans (scan range; 3.0mm, scan resolution; 1000, 100 length) were obtained by the radial scan mode at each time point. We aligned the position of cornea by the real-time display used for guidance (Fig 1A). The position of the cornea was adjusted until the intensity peaks corresponding to the cornea were detected and maximized. The center of the scan pattern was aligned with the corneal vertex reflection [15] visualized on the OCT images (Fig 1B). Corneal epithelial thickness (Epi) and, the total amount of corneal stroma (St) and corneal endothelial thickness (End), were measured by the supplied software (Fig 1C).

Corneal endothelial cell density measurement

In vivo confocal microscopy (IVCM), the Heidelberg Retina Tomograph (HRT) / Rostock Cornea Module (Heidelberg Engineering GmbH, Heidelberg, Germany) was used to examine

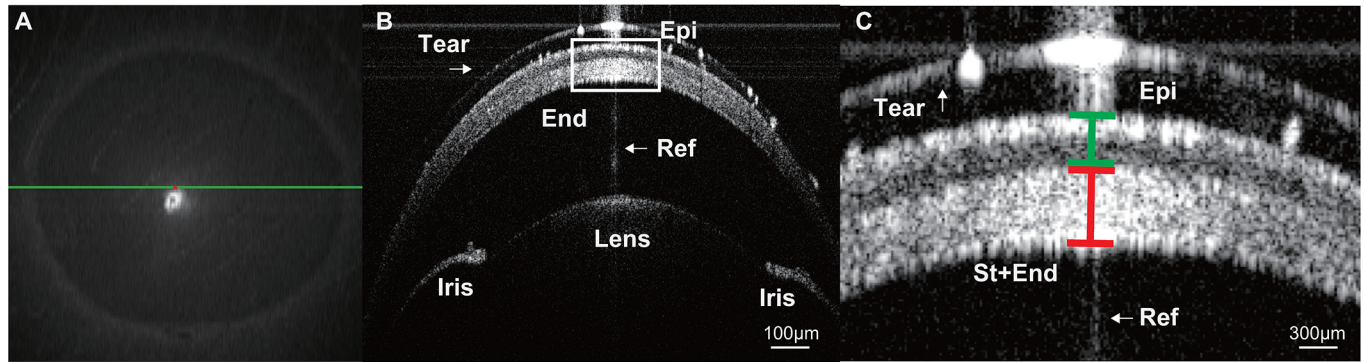


Fig 1. Corneal thickness measurement by AS-OCT. (A) En face projection view (green line shows the position of B-Scan). (B and C) Cross-sectional image of the cornea visualizing different corneal layers (B-Scan). Higher magnification is shown (C). Tear: Tear layer, Epi; Corneal epithelium, Sto: Corneal stroma, End: Corneal endothelium. Ref: corneal vertex reflection.

<https://doi.org/10.1371/journal.pone.0185694.g001>

endothelial cell density (ECD) in the cornea. Mice were anesthetized and placed on the microscope stand and the eyes were coated with Genteal gel (Novartis, St. Louis, MO, USA). Images were taken covering an area of $400 \times 400 \mu\text{m}^2$ and axial optical resolution of $1 \mu\text{m}/\text{pixel}$. Then, ECD areas were analyzed quantitatively using ImageJ.

Corneal fluorescein staining

Corneal fluorescein staining (CFS) and the National Eye Institute grading system (Bethesda, MD) were used to evaluate corneal epithelial damage caused by DED [16]. Briefly, 1 ml of 2.5% fluorescein (Sigma-Aldrich) was applied into the lateral conjunctival sac of the mice and after 3 minutes corneas were examined with a slit lamp biomicroscope under cobalt blue light. Punctate staining was recorded in a masked fashion with the standard National Eye Institute grading system of 0–3 for each of the five areas of the cornea—central, superior, inferior, nasal, and temporal.

Allometric analysis

In allometric analysis, the relationship between the two measured quantities is typically expressed as a power law function which expresses a scale symmetry: $Y = kX^\alpha$, or in a logarithmic form: $\text{Log}(Y) = \alpha \text{Log}(X) + \text{Log}(k)$ [17]. Thus, we fit a linear function to the log/log plot of our data and report the slope, α , as the estimated allometric coefficient.

Statistical analysis

Significance of difference of corneal thickness, body weight and corneal thickness adjusted by weight between different groups were analyzed by one-way ANOVA with Bonferroni post hoc test (Fig 2), and corneal thickness, endothelial cell density and CFS scores were compared to baseline levels by Student's t-test (Fig 3) using Prism software (GraphPad, San Diego, CA, US). Data are presented as mean \pm standard error of mean (SEM) and considered statistically significant at $p < 0.05$. Linear regression analysis and correlation analysis were performed among body weight and corneal thickness using Origin V8.5 SR1 software (OriginLab corporation, Northampton, MA, US) and the built-in statistical packages (Fig 4). Pearson correlation analysis was used for normally distributed data and Spearman correlation analysis was adopted for the abnormally distributed data.

Results

Cornea thickness changes by age

We measured cornea thickness for BALB/c female mice at different ages ranging from one month ($114.7 \pm 3.0 \mu\text{m}$) to 14 months (Fig 2A and 2B). We identified two phases: (i) the thickness increases initially (6 months: $126.3 \pm 1.6 \mu\text{m}$), and then reaches a maximum (9 months: $129.3 \pm 4.4 \mu\text{m}$); (ii) we then observed a reduction in the corneal thickness (12 months: $129.3 \pm 4.4 \mu\text{m}$);

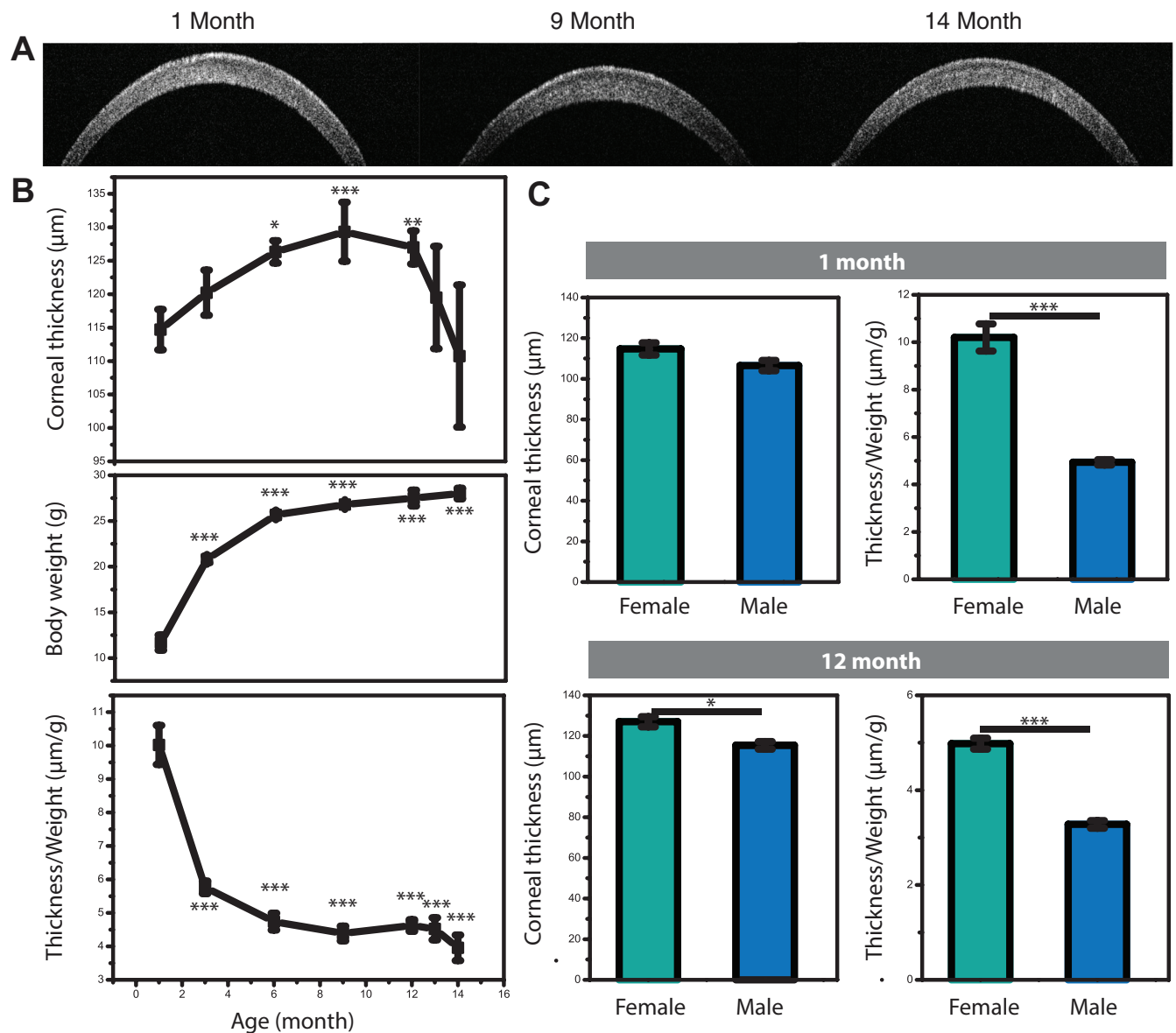


Fig 2. Age-related changes in corneal thickness. (A) Representative OCT images of corneas from female BALB/c mice. (B) Corneal thickness, body weight and corneal thickness/ weight versus age in female BALB/c mice. (C) Corneal thickness depends on sex. Corneal thickness is compared between male and female BALB/c mice. All data were obtained from $n = 10$ mice/group and representative data from three independent experiments are shown. All data were compared to baseline (1 month). p values are calculated using one-way ANOVA with Bonferroni post hoc test, and error bars represent SEM. ($* < 0.05$, $** < 0.01$, $*** < 0.001$).

<https://doi.org/10.1371/journal.pone.0185694.g002>

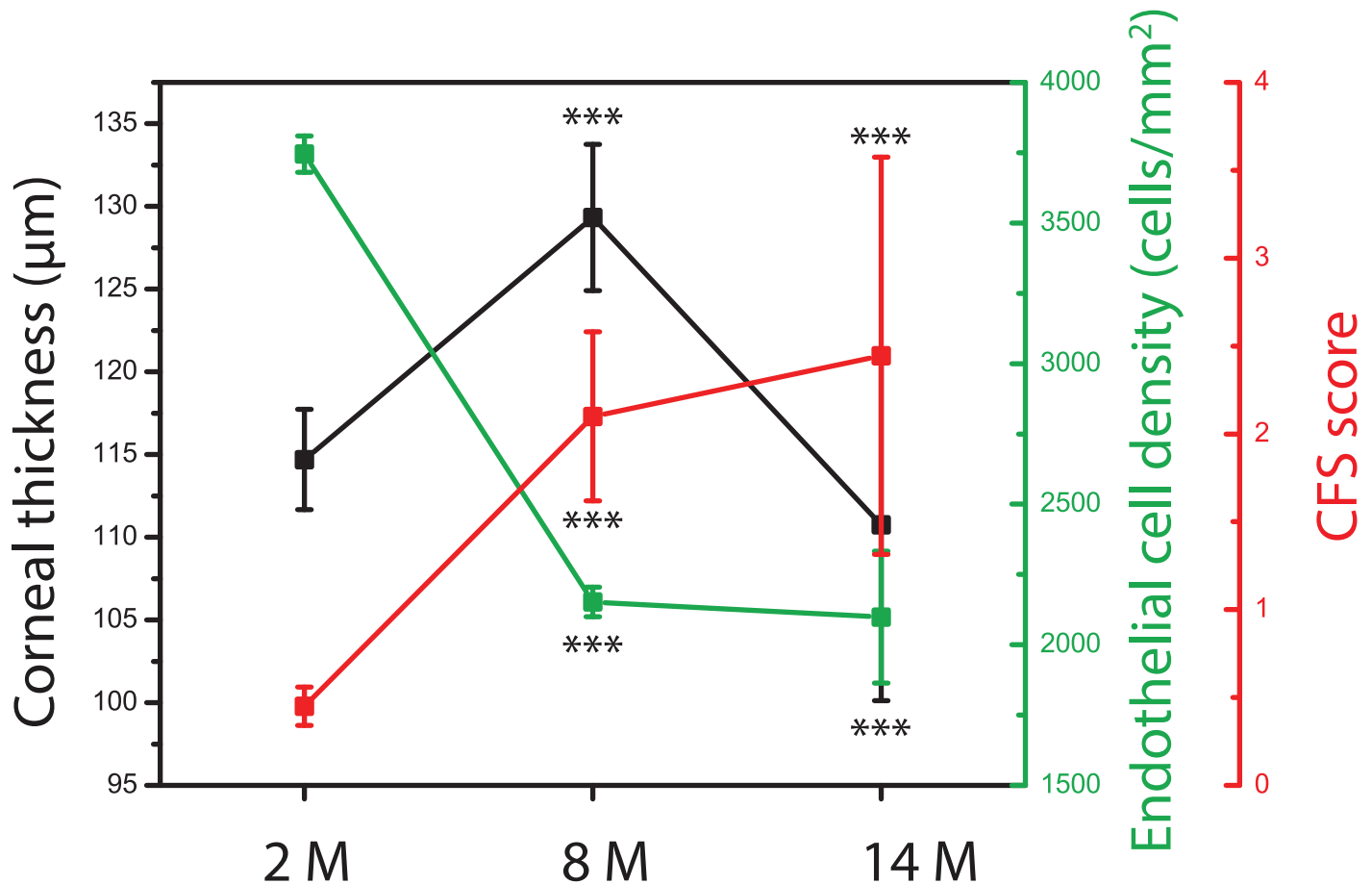


Fig 3. Correspondence between corneal thicknesses and the status of corneal epitheliopathy and endothelial cell layers. The data suggest that, initially, aging affects corneal thickness by changing the boundary layers that maintain the homeostasis of corneal water and electrolytes. Endothelial cell density (ECD) reduces as the mice age from 2M old to 8M old and epithelial layer accumulates damages within this time frame. We have not seen significant changes in corneal epitheliopathy and ECD (contrary to thickness data), when we assessed very old mice (14M). All data were obtained from n = 10 mice/group and representative data from three independent experiments are shown. All data were compared to baseline (2 months). We used female BALB/c mice for this analysis. *p* values are calculated using the Student's t-test and error bars represent SEM. (***) <math>p < 0.001</math>.

<https://doi.org/10.1371/journal.pone.0185694.g003>

127 ± 2.9 µm, 13 months: 119.5 ± 7.6 µm, 14 months: 110.6 ± 10.6 µm). The body size (weight) showed a distinct trend (Fig 2B). For young ages, we observed an increase in the body weight by age that saturates at nearly 6 months (1 month: 11.7 ± 0.6 g, 3 month: 20.8 ± 0.3 g, 6 month: 25.5 ± 0.3 g, 9 months: 27.8 ± 0.7 g, 12 month: 27.5 ± 0.9 g, 13 month: 26.5 ± 0.9 g, 14 month: 28.0 ± 0.6 g). Weight normalized thickness (Fig 2B) follows a trend comprised of an initial decline (1 month: 10.0 ± 0.6 µm/g, 3 month: 5.7 ± 0.2 µm/g, 6 month: 5.0 ± 0.1 µm/g, 9 months: 4.5 ± 0.2 µm/g), a plateau and a decline after one year (12 month: 4.5 ± 0.2 µm/g, 13 month: 4.5 ± 0.3 µm/g, 14 month: 4.0 ± 0.4 µm/g).

We then assessed the contributions of different cornea layers to the overall thickness change. We observed that stroma and endothelium contribute to the thickness change during adulthood and also late in life (S1 Fig). Finally, we assessed epithelial integrity and ECD to see whether age-related changes of corneal thickness are correlated with structural changes of the boundary epithelial and endothelial layers (Fig 3 and Panels A-C in S2 Fig). Initially, aging affects corneal thickness by changing the boundary layers that maintain the homeostasis of corneal water and electrolytes. ECD reduces as the mice age from 2 months to 8 months (2

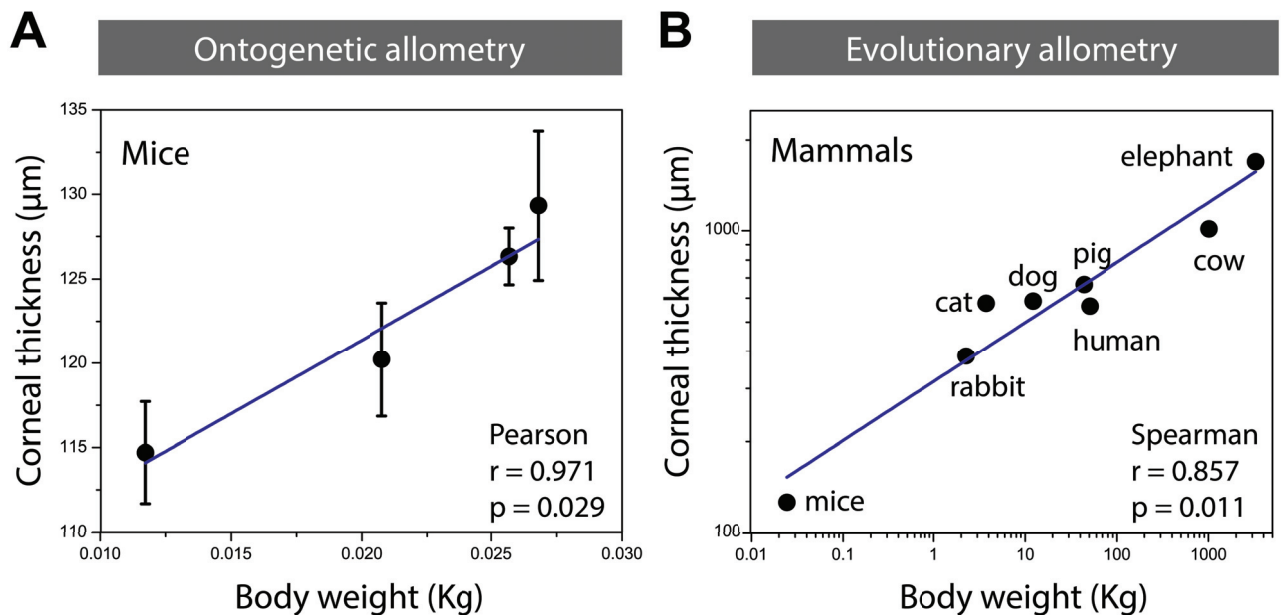


Fig 4. Allometric scaling for corneal thickness. (A) Allometric scaling analysis of 6-month-old female BALB/c mice. Pearson correlation coefficient was used. (B) Evolutionary allometric scaling of adult mammals ($\alpha = 0.2 \pm 0.02$), calculated from reported data for mice, rabbit, cat, dog, pig, human, cow and elephant. Linear regression analysis and correlation analysis were performed among body weight and corneal thickness. Spearman correlation coefficient was used. Pearson correlation analysis was used for normally distributed data and Spearman correlation analysis was adopted for the abnormally distributed data.

<https://doi.org/10.1371/journal.pone.0185694.g004>

months: 3745.3 ± 64.8 cells/ mm^2 , 8 months: 2310.8 ± 46.7 cells/ mm^2) and epithelial layer accumulates damages within this time frame (2 months: 0.5 ± 0.1 , 8 months: 2.1 ± 0.5 , 14 months: 2.4 ± 1.1). Contrary to thickness data, we have not seen significant changes in corneal epitheliopathy and ECD (14 months: ECD; 2098.3 ± 234.5 cells/ mm^2), when we assessed very old mice (14M).

Next we asked if corneal thickness depends on sex and strain. We compared the corneal thickness of 1-month old mice and we observed no difference between the two sexes (Fig 2C). However, for 1-year-old mice we observed significantly thinner cornea in male animals. The difference between sexes became clearer when we normalized the thickness by body weight. To determine if mice of different strains differ in their corneal thickness, we studied two aged- and sex-matched strains, BALB/c and C57BL/6J mice. We observed no significant difference in corneal thickness between the two strains initially, but after normalizing the thickness with body weight, we found that C57BL/6J mice have relatively thinner corneas for their body size (S3 Fig).

Boundary epithelial and endothelial layers change with age

To gain mechanistic insights into the dynamics of corneal thickness, we measured ECD (Panels A and B in S2 Fig). We observed that the density declines fast after one month for several weeks and then continuously decreases with a relatively lower rate for young adults until 14 months. We then normalized the density values with weight and observed that the weight-normalized thickness initially declines and then reaches a plateau at 5–6 months of age.

Next, we asked if animals with different gender differ in their ECD (Panel C in S2 Fig). We compared the ECD of 1-month old female and male mice and we observed no differences. For 1-year old mice, we observed a lower ECD for male mice as compared to the female ones. Normalizing the density values with weight, we found more dramatic difference between the

genders. The male animals, both 1-month and 1-year old, had lower densities when compared to their aged-matched female counterparts.

To gain further mechanistic insights into the dynamics of corneal thickness, we measured epithelial integrity of mouse cornea and its dependency on age (Fig 3). Using CFS and slit lamp assessment, we found that the integrity of corneal epithelium is significantly impaired in 8-month old mice irrespective of gender. The corneal epithelial lining of young adult mice (2-month old) was found to be typically intact.

Evolutionary allometry of cornea

We compared murine corneal thickness with that of other mammals with different body sizes (evolutionary allometric analysis). We extracted central cornea thickness of adult elephant, human, pig, cow, cat, dog, rabbit, and mice [18–25] as well as their reported body weights [20, 21, 23–28] from the literature, and performed allometric analysis (Fig 4). We found that the log-log plot of the corneal thickness versus body weight shows a linear trend. We extracted the allometric coefficient by fitting a linear function to the log-log plot.

Discussion and conclusions

In this study, we measured central corneal thickness changes with age, assessed the dependence of corneal thickness on sex in young and old mice, and compared murine corneal thickness with that of other mammals. The latter provided us with a scaling relation which in turn provides us with a simple way to estimate weight/age dependency of corneal thickness in other animals by only knowing it for mice and without directly measuring it for other animals (which might be practically very difficult for certain rare species).

The changes of corneal thickness by age were still unclear in human and animals. Previous studies reported that there was no significant change in the corneal thickness over time [29, 30] and the others showed the decreased trend of corneal thickness by age [31, 32]. However, those studies did not adjust the measured thicknesses by study subjects' body sizes (weights), which is what we performed in our study (Fig 2). The thickness has a seemingly increasing trend in younger phase [33], which follows by a decreasing trend (Fig 3), but after adjusted by weight, we clearly showed the central corneal thickness has a decreasing trend by age.

The increase in corneal thickness in old mice (8 month old) as compared to young mice (2 month old) was associated with increase in epitheliopathy and decrease in ECD (Fig 3). The changes in epithelial and endothelial function may explain, at least partially, the observed changes in corneal thickness because epithelium and endothelium maintain the hemostasis of water and materials [34] in the cornea. Due to age related changes in these layers, flux of water and materials will likely change and a new steady state and a new corresponding thickness may be reached. Our study however does not provide any functional analysis of epithelial and endothelial layer and these possible scenarios are to be tested in future studies.

To compare corneal thickness from other inbred strains of mice, we measured the central cornea thickness of both BALB/c and C57BL/6J mice (S3 Fig). Our study showed that the murine central corneal thickness was highly strain-dependent. Our data supported previous studies demonstrating that the central corneal thickness of C57BL6J mice was thinner than that of BALB/c mice under weight adjustment [25]. In addition, we revealed ECD was also strongly influenced by genetic backgrounds, suggesting that the genes may influence the physiologic attrition of ECD. Our data has great potential to increase our understanding of the ECD disorder.

This study has some limitations that should be noted. First, we only used AS-OCT for assessing corneal thickness. For accurate examination, it is preferable to evaluate corneal

thickness with various machines such as AS-OCT [15] and Pentacam Scheimpflug system [35]. In clinical setting for human, previous study has reported the comparison between AS-OCT and Pentacam Scheimpflug system for assessing corneal thickness, reporting that AS-OCT and Pentacam are both reliable and reproducible for measuring corneal thickness [36], therefore we examined mice cornea thickness by AS-OCT in this study. Moreover, CFS score was used for assessing corneal epitheliopathy in this study. Although we did not evaluate the corneal structural changes by histological assessment, CFS score was used historically for the evaluation of corneal epitheliopathy for the ocular surface disease such as dry eye disease [37], which is strong correlation with aging [38–41]. Therefore, we consider CFS score was useful for assessing corneal surface epitheliopathy by aging in murine model. Finally, this study was focused on corneal thickness and not cornea size. The thickness is only a partial measure of cornea size. Allometric scaling however can be done for any length scale in our body including limb length and corneal thickness as reported in this article.

Our study has revealed dynamics of corneal thickness during the lifetime of laboratory mouse. Our study will be of interest to researchers studying aging, comparative ophthalmology and veterinary medicine. To extrapolate the results of pharmacological studies performed on mice to other animals, it is essential to understand relevant scaling relations. This is important not only for human studies but also for designing drug therapy for rare animals.

Supporting information

S1 Fig. Thickness of epithelium and, stroma and endothelium combined versus age. Female BALB/c mice were used for the OCT measurements. All data were obtained from $n = 10$ mice/group and representative data from three independent experiments are shown. All data were compared to baseline (1 month). p values are calculated using the Student's t-test and error bars represent SEM. ($* < 0.05$). The left panel presents the full cornea thickness, which is split into two parts, thickness of epithelium and, thickness of stroma and endothelium combined in the right panel.
(EPS)

S2 Fig. Age-related changes in endothelial cell density (ECD). (A) Representative HRT images of corneal endothelial layers from female BALB/c mice. (B) Corneal ECD versus age in female BALB/c mice. (C) Dependency of ECD on sex. Corneal ECD is compared for male and female BALB/c mice. All data were obtained from $n = 10$ mice/group and representative data from three independent experiments are shown. All data were compared to baseline (1 month). p values are calculated using one-way ANOVA with Bonferroni post hoc test, and error bars represent SEM. ($*** < 0.001$).
(EPS)

S3 Fig. Corneal thickness and ECD are compared for BALB/c and C57BL/6J mice. The results of OCT and HRT measurements for the two strains of mice are presented. 12-month old male animals were used for this analysis. All data were obtained from $n = 10$ mice/group and representative data from three independent experiments are shown. p values are calculated using the Student's t-test and error bars represent SEM. ($*** < 0.001$).
(EPS)

Acknowledgments

We thank Dr. Susanne Eiglmeier and Dr. Afsaneh Amouzegar for their editorial assistance with the manuscript.

Author Contributions

Conceptualization: Takenori Inomata, Alireza Mashaghi, Jiaxu Hong, Reza Dana.

Data curation: Takenori Inomata, Takeshi Nakao.

Formal analysis: Takenori Inomata, Alireza Mashaghi.

Funding acquisition: Reza Dana.

Investigation: Takenori Inomata, Takeshi Nakao.

Project administration: Takenori Inomata, Alireza Mashaghi.

Resources: Jiaxu Hong.

Supervision: Reza Dana.

Visualization: Alireza Mashaghi.

Writing – original draft: Takenori Inomata, Alireza Mashaghi.

Writing – review & editing: Reza Dana.

References

1. Edgar BA. How flies get their size: genetics meets physiology. *Nat Rev Genet.* 2006; 7(12):907–16. <https://doi.org/10.1038/nrg1989> PMID: 17139322
2. West GB, Savage VM, Gillooly J, Enquist BJ, Woodruff WH, Brown JH. Physiology (communication arising): Why does metabolic rate scale with body size? *Nature.* 2003; 421(6924):713–.
3. Darveau C-A, Suarez RK, Andrews RD, Hochachka PW. Allometric cascade as a unifying principle of body mass effects on metabolism. *Nature.* 2002; 417(6885):166–70. <https://doi.org/10.1038/417166a> PMID: 12000958
4. Haskell JP, Ritchie ME, Olf H. Fractal geometry predicts varying body size scaling relationships for mammal and bird home ranges. *Nature.* 2002; 418(6897):527–30. <https://doi.org/10.1038/nature00840> PMID: 12152078.
5. Sheridan JA, Bickford D. Shrinking body size as an ecological response to climate change. *Nature Clim Change.* 2011; 1(8):401–6. <http://www.nature.com/nclimate/journal/v1/n8/abs/nclimate1259.html—supplementary-information>.
6. Siemann E, Tilman D, Haarstad J. Insect species diversity, abundance and body size relationships. *Nature.* 1996; 380(6576):704–6.
7. Gomer RH. Not being the wrong size. *Nat Rev Mol Cell Biol.* 2001; 2(1):48–55. <https://doi.org/10.1038/35048058> PMID: 11413465
8. Stanger BZ, Tanaka AJ, Melton DA. Organ size is limited by the number of embryonic progenitor cells in the pancreas but not the liver. *Nature.* 2007; 445(7130):886–91. http://www.nature.com/nature/journal/v445/n7130/supinfo/nature05537_S1.html. <https://doi.org/10.1038/nature05537> PMID: 17259975
9. Stevens CF. Control of organ size: development, regeneration, and the role of theory in biology. *BMC biology.* 2015; 13:14. <https://doi.org/10.1186/s12915-015-0123-7> PMID: 25706761; PubMed Central PMCID: PMC4334576.
10. Shingleton A. Allometry: The Study of Biological Scaling. *Nature Education Knowledge* 2010; 3(10):2.
11. Howland HC, Merola S, Basarab JR. The allometry and scaling of the size of vertebrate eyes. *Vision research.* 2004; 44(17):2043–65. <https://doi.org/10.1016/j.visres.2004.03.023> PMID: 15149837.
12. Ha Tae Song YJK, Soo Jung Lee, Yeon Sung Moon. Relations between Age, Weight, Refractive Error and Eye Shape by Computerized Tomography in Children. *Korean J Ophthalmol.* 2007; 21(3):163–8. <https://doi.org/10.3341/kjo.2007.21.3.163> PMID: 17804923
13. Vaughan D, Asbury T, Lange Medical Books/McGraw-Hill. Vaughan & Asbury's general ophthalmology. New York: Lange Medical Books/McGraw-Hill; 2004. p. v.
14. Bekerman I, Gottlieb P, Vaiman M. Variations in eyeball diameters of the healthy adults. *J Ophthalmol.* 2014; 2014:503645. <https://doi.org/10.1155/2014/503645> PMID: 25431659; PubMed Central PMCID: PMC4238270.
15. Chou TH, Kocaoglu OP, Borja D, Ruggeri M, Uhlhorn SR, Manns F, et al. Postnatal elongation of eye size in DBA/2J mice compared with C57BL/6J mice: in vivo analysis with whole-eye OCT. *Invest*

- Ophthalmol Vis Sci. 2011; 52(6):3604–12. <https://doi.org/10.1167/iov.10-6340> PMID: 21372015; PubMed Central PMCID: PMC3109044.
16. Lemp MA. Report of the National Eye Institute/Industry workshop on Clinical Trials in Dry Eyes. *CLAO J.* 1995; 21(4):221–32. PMID: 8565190.
 17. Giuseppe Longo MM. *Scaling and Scale Symmetries in Biological Systems. Perspectives on Organisms*: Springer Berlin Heidelberg; 2014. p. 23–73.
 18. Bapodra P, Bouts T, Mahoney P, Turner S, Silva-Fletcher A, Waters M. Ultrasonographic anatomy of the Asian elephant (*Elephas maximus*) eye. *J Zoo Wildl Med.* 2010; 41(3):409–17. <https://doi.org/10.1638/2009-0018.1> PMID: 20945637.
 19. Leung DY, Lam DK, Yeung BY, Lam DS. Comparison between central corneal thickness measurements by ultrasound pachymetry and optical coherence tomography. *Clin Exp Ophthalmol.* 2006; 34(8):751–4. <https://doi.org/10.1111/j.1442-9071.2006.01343.x> PMID: 17073897.
 20. Faber C, Erik S, Prause J.U, Sørensen K.E. Corneal Thickness in Pigs Measured by Ultrasound Pachymetry In Vivo. *Scandinavian Journal of Laboratory Animal Science.* 2008; 35:39–43.
 21. Doughty MJ, Petrou S, Macmillan H. Anatomy and morphology of the cornea of bovine eyes from a slaughterhouse. *Canadian Journal of Zoology.* 1995; 73(11):2159–65. <https://doi.org/10.1139/z95-253>
 22. Gilger BC, Wright JC, Whitley RD, McLaughlin SA. Corneal thickness measured by ultrasonic pachymetry in cats. *Am J Vet Res.* 1993; 54(2):228–30. PMID: 8430933.
 23. Alario AF, Pirie CG. Central corneal thickness measurements in normal dogs: a comparison between ultrasound pachymetry and optical coherence tomography. *Veterinary ophthalmology.* 2014; 17(3):207–11. <https://doi.org/10.1111/vop.12074> PMID: 23763504.
 24. Wang X, Wu Q. Normal corneal thickness measurements in pigmented rabbits using spectral-domain anterior segment optical coherence tomography. *Veterinary ophthalmology.* 2013; 16(2):130–4. <https://doi.org/10.1111/j.1463-5224.2012.01041.x> PMID: 22672083.
 25. Lively GD, Jiang B, Hedberg-Buenz A, Chang B, Petersen GE, Wang K, et al. Genetic dependence of central corneal thickness among inbred strains of mice. *Invest Ophthalmol Vis Sci.* 2010; 51(1):160–71. <https://doi.org/10.1167/iov.09-3429> PMID: 19710407; PubMed Central PMCID: PMC2869057.
 26. Das A, Saini M, Katole S, Kullu SS, Swarup D, Sharma AK. Effect of feeding different levels of wheat roti on nutrient utilization and blood metabolite profile in semi-captive Asian elephants (*Elephas maximus*). *J Anim Physiol Anim Nutr (Berl).* 2015; 99(2):367–78. <https://doi.org/10.1111/jpn.12200> PMID: 24821439.
 27. Launer LJ, Harris T. Weight, height and body mass index distributions in geographically and ethnically diverse samples of older persons. *Ad Hoc Committee on the Statistics of Anthropometry and Aging. Age Ageing.* 1996; 25(4):300–6. PMID: 8831875.
 28. Detweiler KB, Rawal S, Swanson KS, de Godoy MRC. Physical activity level of female and male adult cats before and after running wheel habituation. *J Nutr Sci.* 2017; 6:e17. <https://doi.org/10.1017/jns.2017.19> PMID: 28630694; PubMed Central PMCID: PMC5468736.
 29. Han SB, Ang HP, Poh R, Chaurasia SS, Peh G, Liu J, et al. Mice with a targeted disruption of *Slc4a11* model the progressive corneal changes of congenital hereditary endothelial dystrophy. *Invest Ophthalmol Vis Sci.* 2013; 54(9):6179–89. <https://doi.org/10.1167/iov.13-12089> PMID: 23942972.
 30. Zheng Y, Huang G, Huang W, He M. Distribution of central and peripheral corneal thickness in Chinese children and adults: the Guangzhou twin eye study. *Cornea.* 2008; 27(7):776–81. <https://doi.org/10.1097/ICO.0b013e31816f62d3> PMID: 18650662.
 31. Nemesure B, Wu SY, Hennis A, Leske MC, Barbados Eye Study G. Corneal thickness and intraocular pressure in the Barbados eye studies. *Arch Ophthalmol.* 2003; 121(2):240–4. PMID: 12583791.
 32. Ueno Y, Hiraoka T, Miyazaki M, Ito M, Oshika T. Corneal thickness profile and posterior corneal astigmatism in normal corneas. *Ophthalmology.* 2015; 122(6):1072–8. <https://doi.org/10.1016/j.ophtha.2015.01.021> PMID: 25769847.
 33. Song J, Lee YG, Houston J, Petroll WM, Chakravarti S, Cavanagh HD, et al. Neonatal corneal stromal development in the normal and lumican-deficient mouse. *Invest Ophthalmol Vis Sci.* 2003; 44(2):548–57. PMID: 12556382; PubMed Central PMCID: PMC1853375.
 34. Li LY, Tighe B. Numerical simulation of corneal transport processes. *J R Soc Interface.* 2006; 3(7):303–10. <https://doi.org/10.1098/rsif.2005.0085> PMID: 16849239; PubMed Central PMCID: PMC1578740.
 35. Puk O, de Angelis MH, Graw J. Lens density tracking in mice by Scheimpflug imaging. *Mamm Genome.* 2013; 24(7–8):295–302. <https://doi.org/10.1007/s00335-013-9470-2> PMID: 23929037.
 36. Chen S, Huang J, Wen D, Chen W, Huang D, Wang Q. Measurement of central corneal thickness by high-resolution Scheimpflug imaging, Fourier-domain optical coherence tomography and ultrasound

- pachymetry. *Acta Ophthalmol.* 2012; 90(5):449–55. <https://doi.org/10.1111/j.1755-3768.2010.01947.x> PMID: [20560892](https://pubmed.ncbi.nlm.nih.gov/20560892/).
37. Chen Y, Chauhan SK, Lee HS, Saban DR, Dana R. Chronic dry eye disease is principally mediated by effector memory Th17 cells. *Mucosal Immunol.* 2014; 7(1):38–45. <https://doi.org/10.1038/mi.2013.20> PMID: [23571503](https://pubmed.ncbi.nlm.nih.gov/23571503/); PubMed Central PMCID: PMC3732510.
 38. Den S, Shimizu K, Ikeda T, Tsubota K, Shimmura S, Shimazaki J. Association between meibomian gland changes and aging, sex, or tear function. *Cornea.* 2006; 25(6):651–5. <https://doi.org/10.1097/01.ico.0000227889.11500.6f> PMID: [17077655](https://pubmed.ncbi.nlm.nih.gov/17077655/).
 39. Hykin PG, Bron AJ. Age-related morphological changes in lid margin and meibomian gland anatomy. *Cornea.* 1992; 11(4):334–42. PMID: [1424655](https://pubmed.ncbi.nlm.nih.gov/1424655/).
 40. Schaumberg DA, Dana R, Buring JE, Sullivan DA. Prevalence of dry eye disease among US men: estimates from the Physicians' Health Studies. *Arch Ophthalmol.* 2009; 127(6):763–8. <https://doi.org/10.1001/archophthalmol.2009.103> PMID: [19506195](https://pubmed.ncbi.nlm.nih.gov/19506195/); PubMed Central PMCID: PMC2836718.
 41. Schaumberg DA, Sullivan DA, Buring JE, Dana MR. Prevalence of dry eye syndrome among US women. *Am J Ophthalmol.* 2003; 136(2):318–26. PMID: [12888056](https://pubmed.ncbi.nlm.nih.gov/12888056/).